Development of ideal processing parameters for powder bed fusion system processing of AlSi10Mg using design of experiments

Development of ideal processing parameters for powder bed fusion system processing of AlSi10Mg using design of experiments

N R Mathe*

Laser Enabled Manufacturing Research Group, National Laser Centre, Council for Scientific and Industrial Research, Pretoria 0001, South Africa

E-mail: nmathe@csir.co.za

Abstract. The additive manufacturing of aluminium alloys has gained great interest in the transport industry in the past 10 years. This is mainly due to the lightweight and good strength that these alloys offer especially for applications in aerospace and other related industries. However, there is a drawback in using these alloys especially the parts produced by additive manufacturing as they have to be heat treated before application to relieve residual stresses caused by the fast heating and cooling experienced during powder bed fusion (PBF) fabrication. Most of the current PBF metal system offer a variety of processing parameters for part building, however AM uptake and industrial implementation is still slow due to restrictions of the laser power and laser interaction time that are slow and thus the parts take long to produce. Seeing this lag in the market, the CSIR has produced a high speed and high power PBF machine with a build platform larger than the currently available commercial systems. This system allows for the faster production of parts due to its higher consolidation rate and it has already been validated for aluminium alloys, specifically AlSi10Mg. The properties evaluated were microstructure and hardness, which found to be comparable to commercial PBF machines. The samples were analysed for microstructure, mechanical properties using tensile testing procedure. In order to determine that ideal processing window, the response surface methods was used on the Stat-Ease Design Expert software using ultimate tensile strength, elongation and hardness as outputs. Based on the data analysed, the processing window was narrowed to 1400 W laser power and 1.63 – 1.95 s interaction time.

1. Introduction

Aluminum alloys are widely used material sin industrial applications such as aerospace, rail and automotive part manufacturing. This is mainly due to its good strength and light weight that leads to an increase in fuel efficiency for the transport industry. Although this metal has been produced by casting and other traditional methods, there has been an increase in the additive manufacturing of these alloys. Additive manufacturing in this case is attractive as it allows for the production of complex parts.

Although there has been a wider use of Aluminiun in additive manufacturing, more work still needs to be done to understand the impact of processing parameters on the mechanical properties of the samples, especially for new systems that are being produced by 3D printing manufacturers.

In our previous work on AlSi10Mg additive manufacturing, [1], the in-house built powder bed fusion (PBF) system was validated in terms of the consolidation and microstructure that were compared with commercial PBF systems [2, 3]. This current work is a continuation and it aim to develop an ideal

processing window for AlSi10Mg using the laser interaction time, [4], and laser power as input parameters, the outputs are hardness, elongation and UTS. The method of optimization to be employed is the factorial Design of Experiment (DoE) using the Stat-Ease Design Expert software using the surface response method (RSM) [5]. RSM exhibits the factorial contributions from the coefficients using a regressive model, and the configurations are identified using input process variables and responses from experimental data. The RSM in as ideal process that is used to determine the suitability of the selected process parameters and their effects on the response of the designed experiment [5-7].

2. Methodology

2.1. Feedstock and processing

The samples were prepared using spherical AlSi10Mg powder with a particle size distribution of 35 – 60 μm, purchased from TLS Technik GmbH, Germany as it was dried in the oven at 100 degrees Celsius before use, see previous work for powder analysis, [1]. Design of Experiment on the Design Expert software was used to determine the ideal processing parameters. The processing parameters in this work were based on the previous results obtained by the authors. The samples were produced using the CSIR in-house built powder bed fusion system installed with a 3 kW IPG multi-mode fibre laser, 400X360 circular build platform [1]. The laser power and interaction time values were varied.

2.2. Characterization

The cube densities were measured using the Ohaus Meters Densitometer employing the Archimedes principle in ethanol medium. The cube and tensile specimen were produced and characterized for micro-hardness testing that were performed on a Roell micro-Vickers hardness tester (ZHVμ). The 20kN Zwick/ Roell Tensile tester was used applying standard ASTM E8/E8M-16a for tensile strength measurements. The microstructures of the samples were taken on the Olympus BX51M light optical microscope and the JEOL JSM 6010/LA Plus scanning electron microscope. Note: The samples were all tested as-built.

3. Results and Discussion

The results obtained in this work are presented as a function of laser power and laser interaction time. The interaction time was calculated according to the equation by Matilainen et al., [4]. The laser interaction time (s) was based on the ratio between, v is the laser scanning speed (mm/s) and d is the spot size (mm). The actual values were not obtained as they are the proprietary information of the equipment manufacturer.

3.1. Microstructure analysis

The microstructures of the samples were analyzed using the optical and scanning electron microscopes to determine the morphology and surface pores that are present in the samples. The AlSi10Mg cubes samples that were produced on the in-house PBF were mounted and polished in order to analyze the microstructure using SEM (Figure 1) and optical microscopy (Figure 2). In Figure 1, the SEM images were analyzed for surface defects pores as a function of laser power and interaction time. It was observed that, at lower power (1000 W), there we surface defects for all the samples. As the laser power was increased to 1200 and 1400 W, there were less defects however there were clear surface pores. These pores were randomly distributed between the layers and along the melt pool. Aboulkhari et al, [8], and Pei et al., [9], observed that the surface pores increase as they increase the scanning speed for a constant laser power.

Optical micrograph of the samples presented in Figure 2. It can be seen that the scale-pattern morphology that is typical of AlSi10Mg produced by PBF, [1], was not observed for all the samples. In some samples long grains observed. This is a results of the scanning strategy as also observed by Pei et al., [9].

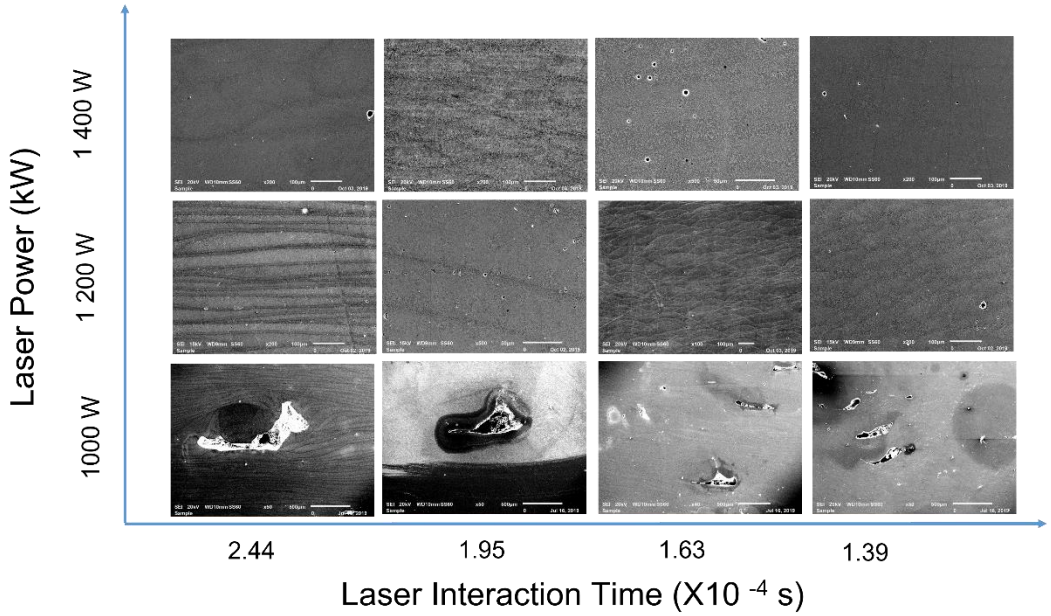

Figure 1. SEM micrographs of AlSi10Mg as a function of processing parameters.(Note: scale bar = 100 µm).

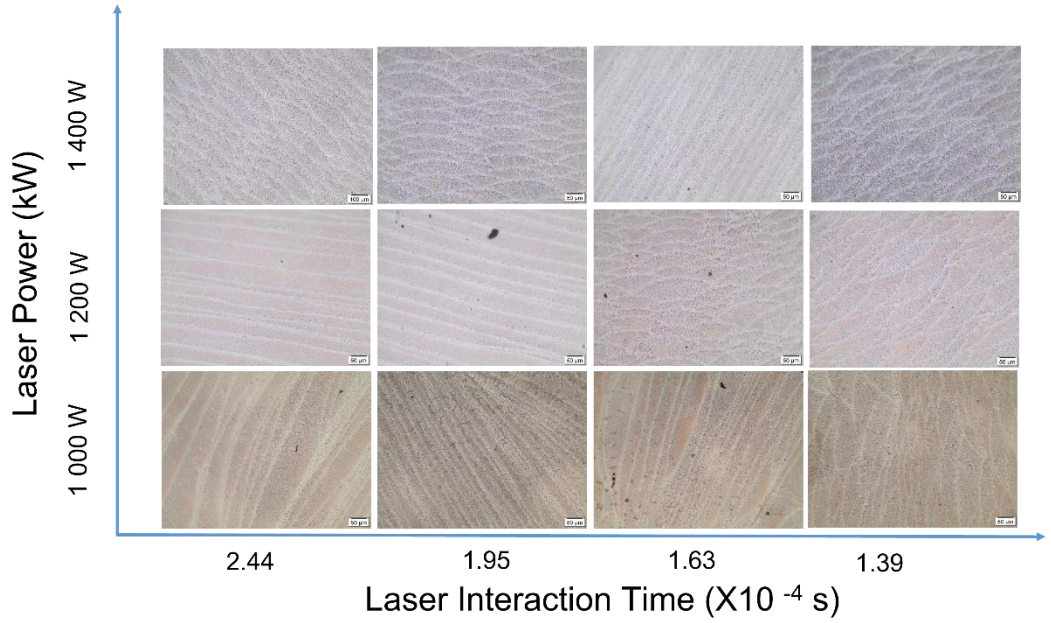

Figure 2. Microstructure morphology of AlSi10Mg samples produced by PBF. (Note: scale bar = 50 µm).

3.2. Static mechanical properties

3.2.1. The tensile properties of the samples are presented in Figure 3. The properties were tested on 5mm and 10 mm length dog-bone specimen with a gauge length of 5mm. The laser power and interaction were the varied parameters in this case. It was observed that there was a change in the ultimate tensile strength (UTS) values presented in Figure 3a with a change in laser power, i.e. the higher the laser power, the higher the UTS value for each interaction time. This was also observed by Read et al, [5] for PBF

processing of AlSi10Mg alloys. This behaviour is attributed to the keyhole pores observed at lower laser powers that affect the load bearing ability of the samples [10]. However, there was no significant change in the UTS as a function of the laser interaction time. The UTS values obtained ranged from 208 – 310 MPa which is comparable to literature SLM values [5, 11], and also comparable to die casted at 300 MPa [5].

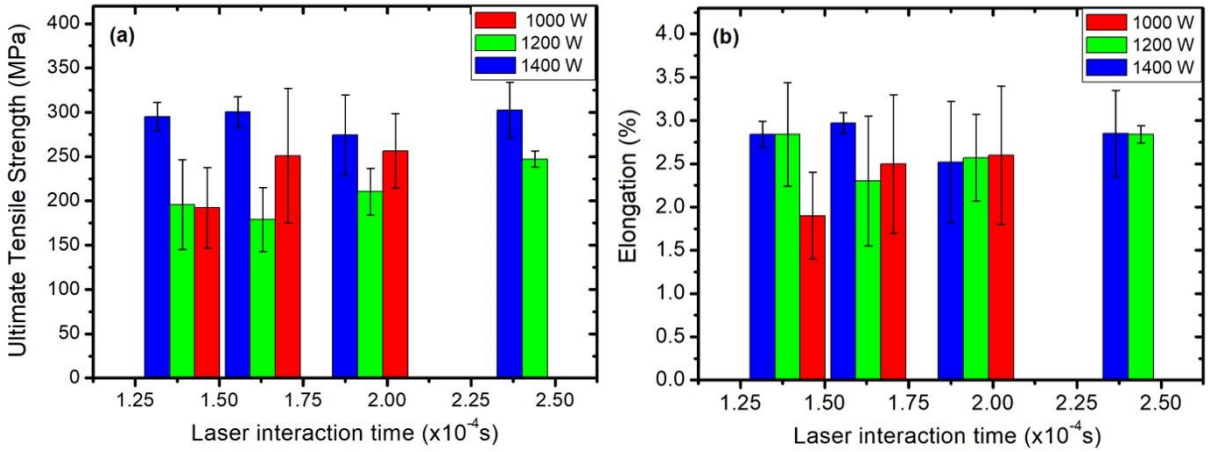

Figure 3. Tensile testing data; (a) UTS and (b) elongation presented as a function of laser power and interaction time.

The elongation of the samples was also determined and plotted as a function of laser power and laser interaction time in Figure 3b. The elongation values obtained in this work ranged from 1.0 – 1.2%, with the 1500 and 1400 W samples exhibiting the higher elongation. These values are significantly lower than what was obtained by other authors in literature for as-built and die casted samples using the same alloy [2, 11, 12].

3.2.2. Vickers Hardness Measurement. The hardness values for the AlSi10Mg samples are presented in Figure 4as a function of laser power and interaction time. There was no significant change in the hardness values as the laser power increased and the values ranged from 125 – 130 Hv. The value are comparable to Kempen et al., [12], Mfusi et al., [2] for commercial PBF processing and lower than the casted value of 74 Hv.

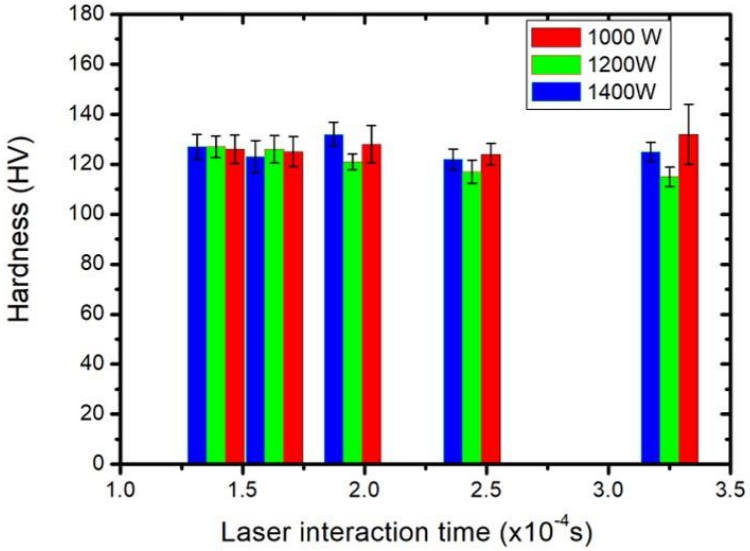

Figure 4. Hardness measurements of AlSi10Mg samples with varied laser power and interaction time.

3.3. Design Expert parameter optimization

The UTS, elongation and hardness values were used to determine the ideal processing parameters window in this work. Table 1 shows the selected processing parameters inputs and outputs using the Stat-Ease Design Expert software.

Table 1. Processing parameters.

Std	Run	Factor 1 A:Laser Power W	Factor 2 B:Laser Interatio... s	Response 1 UTS MPa	Response 2 Elongation %	Response 3 Hardness HV
6	1	1400	0.000244	302.5	2.85	122
8	2	1200	0.000244	247.2	2.84	117
1	3	1000	0.000244	0	0	214
2	4	1400	0.000195	274.5	2.52	132
5	5	1000	0.000195	256.5	2.6	128
3	6	1000	0.000163	250.9	2.5	125
4	7	1400	0.000163	300	2.97	123
7	8	1200	0.000195	210.4	2.57	121
9	9	1000	0.000139	192.1	1.9	126
10	10	1200	0.000163	179	2.3	126
11	11	1200	0.000139	196	2.84	127
12	12	1400	0.000139	295.3	2.84	127

3.3.1. UTS and Elongation output. The response surface plot in Figure 5 shows the change in UTS values as a function on both laser power and laser interaction time. This methods was previously used by Oyesola et al., [6], for surface roughness optimization of Ti6Al4V, and Dada et al., [7], for the optimization of high entropy alloys processing parameters. In this case, the influence of the laser power on the UTS can be clearly seen, where as the laser power increase, the UTS value increased. The higher the laser power, the higher the energy input into the material during processing, thus resulting in increased strength.

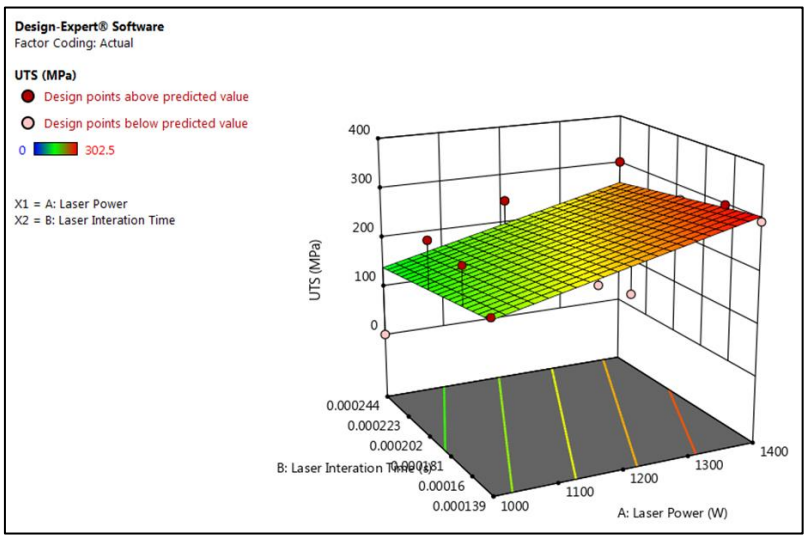

Figure 5. Response surface plot for UTS optimization with varied laser power and interaction time.

The same method was applied for the elongation as an output and the response surface plot is presented in Figure 6. It was observed that as the laser power and the interaction time decreased, the elongation increased.

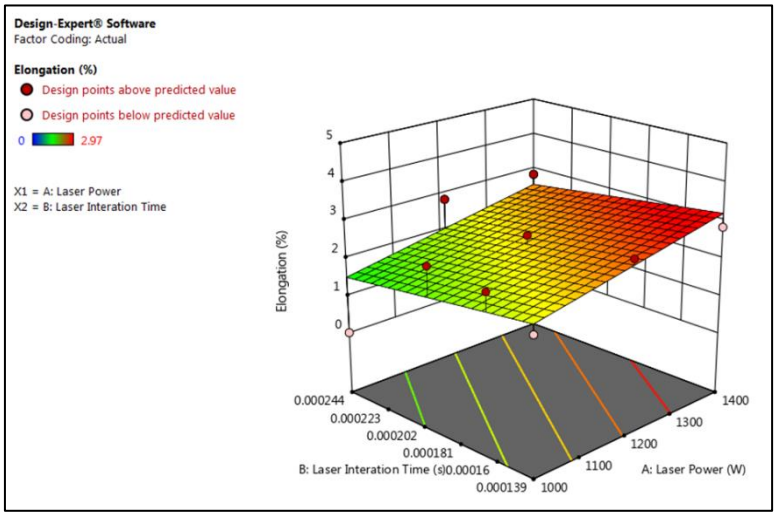

Figure 6. Response surface plot for UTS optimization with varied laser power and interaction time.

3.3.2. Hardness output. The response surface plot of the hardness output as a function of laser power and interaction time in presented in Figure 7. The observation made in this case was that the ideal hardness values were obtained at lower interaction time and high laser powers. This is due to the pores observed in Figure 2 affecting the load bearing of the samples at lower powers and thus decreasing the hardness of the samples [13]. This is contrary to the tensile properties which showed a different trend.

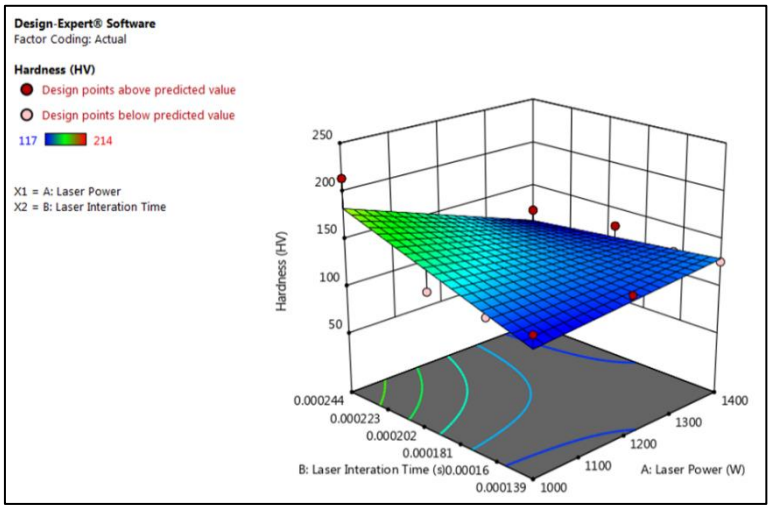

Figure 7. Response surface plot for UTS optimization with varied laser power and interaction time.

4. Conclusion

The AlSi10Mg samples were prepared using the CSIR in-house built powder bed fusion with varied laser power and laser interaction time. The main focus was to determine the ideal processing parameters using design of experiment and response surface methods with UTS, elongation and hardness as the outputs. The SEM results showed that at lower laser powers, there were defects on the surface of the samples, which were not observed for higher laser powers. From SEM analysis, 2 samples showed the least amount of surface pores, namely, 1200W & 1.63×10^{-4} s and 1400W & 1.95×10^{-4} s.

The highest UTS values were observed at 1400 W for all the interaction times, with the highest elongation at 1400 W& 1.93×10^{-4} s. There was no significant change in the hardness values, but at 1400 W the values were generally higher than other samples. This was also confirmed by the response surface plot. Therefore, it can be concluded that the ideal processing parameters for AlSi10Mg using the CSIR

in-house built PBF machine are as follows; laser power of 1400 W and 1.63 – 1.95x10^{-4} s laser interaction time.

References

[1] Mathe N R and Tshabalala L C 2019 The validation of the microstructural evolution of selective laser-melted AlSi10Mg on the in-house built machine: energy density studies *Prog. in Addit. Manuf.* **4**(4) 431-442.
[2] Mfusi B J, Tshabalala L C, Popoola A P I and Mathe N R 2018 The effect of selective laser melting build orientation on the mechanical properties of AlSi10Mg parts *IOP Conf. Series: Mater. Sci. Eng.* **430** 012028.
[3] Brandl E, Heckenberger U, Holzinger V and Buchbinder D 2012 Additive manufactured AlSi10Mg samples using Selective Laser Melting (SLM): Microstructure, high cycle fatigue, and fracture behavior *Mater. Design* **34** 159-69.
[4] Matilainen V P, Piili H, Salminen A and Nyrhilä O 2015 Preliminary Investigation of Keyhole Phenomena during Single Layer Fabrication in Laser Additive Manufacturing of Stainless Steel *Phys. Procedia* **78** 377-387.
[5] Read N, Wang W, Essa K and Attallah M M 2015 Selective laser melting of AlSi10Mg alloy: Process optimisation and mechanical properties development *Mater. Design* **65** 417-424.
[6] Oyesola M, Mpofu K, Mathe N, Fatoba S, Hoosain S and Daniyan I 2021 Optimization of selective laser melting process parameters for surface quality performance of the fabricated Ti6Al4V *Int. J. Adv. Manuf. Tech.* **114**(5) 1585-99.
[7] Dada M, Popoola P, Mathe N, Pityana S and Adeosun S 2020 Parametric optimization of laser deposited high entropy alloys using response surface methodology (RSM) *Int. J. Adv. Manuf. Tech.* **109**(9) 2719-32.
[8] Aboulkhair N T, Everitt N M, Ashcroft I and Tuck C 2014 Reducing porosity in AlSi10Mg parts processed by selective laser melting *Addit. Manuf.* **1–4** 77-86.
[9] Wei P, Wei Z Y, Chen Z, Du J, He Y Y, Li J F and Zhou Y T 2017 The AlSi10Mg samples produced by selective laser melting: single track, densification, microstructure and mechanical behavior *Appl. Surf. Sci.* **408** 38-50.
[10] Bai S, Perevoshchikova N, Sha Y and Wu X 2019 The Effects of Selective Laser Melting Process Parameters on Relative Density of the AlSi10Mg Parts and Suitable Procedures of the Archimedes Method *Appl. Sci.* **9**(3) 583.
[11] Rosenthal I, Stern A and Frage N 2014 Microstructure and Mechanical Properties of AlSi10Mg Parts Produced by the Laser Beam Additive Manufacturing (AM) Technology *Metallogr. Microst. Anal.* **3**(6) 448-53.
[12] Kempen K, Thijs L, Van Humbeeck J and Kruth J P 2012 Mechanical Properties of AlSi10Mg Produced by Selective Laser Melting *Phys. Procedia* **39** 439-46.
[13] Wu H, Ren Y, Ren J, Liang L, Li R, Fang Q, Cai A, Shan Q, Tian Y and Baker I 2021 Selective laser melted AlSi10Mg alloy under melting mode transition: Microstructure evolution, nanomechanical behaviors and tensile properties *J. Alloy. Compd.* **873** 159823.